ChemCatChem

Research Article
doi.org/10.1002/cctc.202300716

Chemistry Europe
European Chemical Societies Publishing

www.chemcatchem.org

VIP *Very Important Paper*

Special Collection

Desilicated ZSM-5 Catalysts: Properties and Ethanol to Aromatics (ETA) Performance

Daniel Dittmann,[a] Elif Kaya,[a] and Michael Dyballa*[a]

Herein, desilication in increasingly harsh conditions was used to introduce mesopores into two different industrial ZSM-5 catalysts (Si/Al ratio 11 or 29). For desilicated samples, increasing BET surface areas, mesopore volumes, and Si(OH) densities were noted. Brønsted acid site (BAS) densities increased upon desilication, as formerly inaccessible BAS in blocked pores became available, while the strength of the BAS was maintained upon desilication. Using KOH instead of NaOH as desilication agent can increase the mesopore volume generated per mass loss. The correlations between desilication strength and properties were largely determined by the parent Si/Al ratio. In general the introduced mesopores increased lifetimes in the ETA conversion, while additional Si(OH) groups introduced by desilication reduce the lifetime again. The lifetime is thus determined by a complex interplay of BAS density, improved reactant transport by introduced mesopores and Si(OH) density. There were no additional aromatics formed in desilicated samples during the conversion of ethanol and the samples were, in terms of aromatic yield, outperformed by a microporous parent. However, as result of longer lifetimes less ethanol was lost due to coke formation. It is concluded that desilication should be combined with other post-modifications to increase aromatic production and lifetime.

Introduction

The platform for today's production of base chemicals and fuels is fossil oil and gas. However, the current regulation makes this platform increasingly unattractive for investments. Ethanol could be an alternative, bio-based platform chemical in years to come. Whereas nowadays the main amount of ethanol is used as additive for car fuel, in future these production capacities become available for example for the production of jet fuel.[1] To increase the generated value, ethanol could also be used as an alternative platform chemical for the chemical industry. Aromatics for example can nowadays be cheaply extracted from product streams during the conversion of fossil oil.[2] Few alternatives exist to this route, despite a direct route to aromatics could become increasingly important when the amount of oil converted by refineries decreases and cheap alternatives to generate aromatics vanish. A potential route is hydrodeoxygenation of lignin-derived biomass.[3] Likewise, the conversion of methanol-to-X (X = aromatics), could be applied.[4] However, methanol is in large scales nowadays only produced from fossil sources.[5] An alternative based on a "renewable" feedstock is the direct conversion of ethanol-to-aromatics (ETA) that is usually conducted over 10-membered ring zeolites like ZSM-5. Thereby Brønsted acid sites (BAS) in form of bridging Si(OH)Al groups are the catalytically active sites. Initial mechanistic interpretations, for example by Derouane et al.,[6] found a close relation between the conversion of methanol and ethanol. However, in recent years it was shown that significant differences exist. For example, the initial dehydration of ethanol to ethylene is mechanistically separated from subsequent reaction steps.[7] Obviously, in contrast to methanol feed, in the ethanol feed the first carbon-carbon bond is already immanent. This has large impacts on secondary reactions, as for ethanol the subsequent homologation of ethylene and cracking steps are far more important than for methanol feed. Remarkably, these intermediates and products, for example propylene, have not necessarily an even carbon number. This can be rationalized with the presence of surface methoxy groups (SMG) that lead in consequence to the parallel appearance of reaction cycles known from methanol-to-olefins conversion, were recently identified.[8] The immediate dehydration of ethanol feed to ethylene makes also adjustments of the feed more promising, because unneeded water can be efficiently removed initially which enables longer lifetimes and higher aromatic yields.[9]

Due to the mentioned chemical and mechanistic differences between ethanol and methanol feeds it is highly interesting if post-modifications that are frequently applied for ZSM-5 catalysts in methanol conversion have also beneficial effects on the ETA catalysts. Typical post-modifications applied to zeolites are the phosphatation,[10] dealumination,[11] both applied to alter the acidity of zeolites, and finally desilication,[10e,12] whereby both diffusion and acid properties of zeolite catalyst can be varied. As the most interesting aromatics for industry (benzene, toluene, ethylbenzene, and xylenes; abbreviated BTEX) tend to

[a] *D. Dittmann, E. Kaya, Dr. M. Dyballa*
Institute of Technical Chemistry
University of Stuttgart
Pfaffenwaldring 55
70569 Stuttgart (Germany)
E-mail: michael.dyballa@itc.uni-stuttgart.de
Homepage: www.mdyballa.de

Supporting information for this article is available on the WWW under https://doi.org/10.1002/cctc.202300716

This publication is part of the Catalysis Talents Special Collection. Please check the ChemCatChem homepage for more articles in the collection.

© 2023 The Authors. ChemCatChem published by Wiley-VCH GmbH. This is an open access article under the terms of the Creative Commons Attribution License, which permits use, distribution and reproduction in any medium, provided the original work is properly cited.

© 2023 The Authors. ChemCatChem published by Wiley-VCH GmbH

block the pores of ZSM-5 and are thus coke precursors, it is reasonable that better accessibility by more pore openings and mesoporous "highways" could be a well-suited post-modification route.[13] It should be noted that even longer lifetimes in methanol conversion, compared to "classical" micro-/mesoporous ZSM-5 derived from desilication, can be achieved by adding additional macropores into the ZSM-5 framework.[12a]

A desilication of zeolites obviously removes silicon from the zeolite framework. Such dissolved crystal fragments are usually visible in SEM pictures.[12c] However, in contrast to the framework silicon the aluminum remains not in form of bridging Si(OH)Al groups within the framework of desilicated zeolites but is released from the latter and thus rather an amorphous deposit. The balance between silicon dissolution and aluminum deposition is the reason for a changing BAS density in many reports on desilicated zeolites.[11c,12b,f–h,14] An acid wash following the desilication in alkaline media can remove potentially deposited extra-framework aluminum in order to preserve the parents crystallinity and BAS density.[15] The sodium cations from the NaOH solution applied during desilication or extracted aluminum cations could also remain after desilication in counter ion position, thereby changing the BAS density and reactivity of catalysts.[16] Thus both an acid wash, often with HCl, or a subsequent ion exchange with aqueous NH_4NO_3[12i] also serve the purpose to exchange Na-forms of BAS into the catalytically active H-form. If this wash is skipped, blocked pores and varying, hardly predictable acid properties of the mesoporous ZSM-5 might be caused.[12b]

As a harsh dissolution might overcompensate for the positive effect of introducing mesopores by decreasing crystallinity or complete collapse of the framework, aqueous NaOH concentrations of 1 M and above should be avoided.[12c] Conclusively, the selectivity to aromatics during methanol conversion over desilicated ZSM-5 runs often through an optimum with respect to desilication strength.[11d,12h] There are indications that initially present defects might play a major role for where and how strong desilication dissolves the framework.[12b,17] Defect sites, resulting from the uncontrolled dissolution of the ZSM-5 framework, were reported to increase the amount of aromatics and lifetime in the methanol conversion.[18] It was also reported that the total Si(OH) density is increased upon desilication.[17,18b] During methanol conversion mesoporous ZSM-5 catalysts had a homogeneous coke deposition and deactivation compared to the unmodified parent.[12i] It is also known that the coke composition depends strongly on the size and morphology of the sample.[19] Thus it can be stated that the initially used ZSM-5 parent defines largely how desilication changes the parent's catalytically relevant properties for the conversion of methanol.

Whereas desilicated samples were frequently used for the conversion of methanol, studies involving desilication and ethanol conversion to aromatics or other hydrocarbons are scarce. Most studies deal with ethanol dehydration. The mechanism of the dehydration step was recently described applying solid-state NMR.[20] Desilicated ZSM-5 was used as promising catalyst for ethanol dehydration to ethylene or diethyl ether.[21] Lakiss et al.[19] applied differently shaped and subsequently desilicated ZSM-5 catalysts in the ethanol-to-hydrocarbon conversion at 623 K and overpressure (3 MPa). A detailed IR characterization of catalyst acidity, also involving the generation of BAS on the external surface or in newly generated mesopores, was conducted. The introduction of more pore mouths and generation of shorter diffusion path lengths to the external ZSM-5 surface was identified as mechanistic explanation for the strongly enhanced lifetime upon desilication. Nanosized parents behave nearly as desilicated post-modifications. Only the lifetimes of very large parent crystallites were strongly improved. The low yield of alkanes in the gaseous fraction indicates a similarly low yield of stoichiometrically formed aromatics in a study applying an even higher overpressure.[22] Nevertheless, a higher selectivity to C_4–C_9 hydrocarbons, compared with microporous ZSM-5, was noted after desilication. For dealuminated and base-washed ZSM-5 catalysts applied in the ethanol conversion, it was found that the location and thus shape-selectivity of BAS sites, causing different reaction speeds, in combination with the speed of transport determine how many aromatics are formed and how fast ZSM-5 catalysts deactivate.[11e,f] Jun et al.[23] reported an increased formation of aromatics and lifetime upon desilication of a ZSM-5. The authors suggested that the mesopore diameter were relevant for the catalytic aromatization. As these previous studies often applied largely different ZSM-5 parents, often from laboratory synthesis and in μm-size, herein typical industrial material is utilized as parent for revealing the impact of desilication on the ETA conversion performance. Therefore, synthesis and thorough characterization of two families of desilicated catalysts based on two industrially available ZSM-5 parents was conducted. Catalytic measurements reveal how these properties impact the ETA conversion product composition and lifetime.

Results and Discussion

Physicochemical characterization of materials

Physicochemical properties of materials before and after post-modification by desilication were evaluated by standard techniques and results are summarized in Table 1. The sample nomenclature reflects the desilication strength, whereby harshest desilication is represented by a later alphabetical letter and a decreasing yield after desilication treatment (*vide supra*). In general, desilication leads to significant decreases in the mass of the catalysts as large parts of the solid are dissolved. Even soft desilication leads to a loss of about 20 or 25 % of the parent ZSM-5 mass, respectively. The amount of dissolved ZSM-5 matter is thereby, in agreement with literature, depending on the Si/Al ratio of the parents.[12e] The desilication efficiency, as measure of the introduced mesopore volume per dissolved catalysts mass, is highest for the samples derived from the Si/Al = 11 parent, S11. Chemical analysis shows an increasing Si/Al ratio upon desilication for post-modified samples derived from S11. This agrees with literature results for combined NaOH/HCl treatments on a ZSM-5 parent of this Si/Al ratio.[11e] We find a

© 2023 The Authors. ChemCatChem published by Wiley-VCH GmbH

Table 1. Data from the physicochemical characterization of the materials under study.

Material	Si/Al ratio[a)]	Crystallinity [%][b)]	BET surface [m^2/g][c)]	V_{meso} [mL/g][c)]	Si(OH) density [mmol/g][d)]	BAS density [mmol/g][e)]	External BAS density [mmol/g][f)]
S11	11	90	420	0.14	0.16	0.66 (+0.22)[g)]	none
S11/A	15	90	420	0.23	0.13	1.00	0.01
S11/B	14	70	460	0.32	0.29	0.66	0.02
S11/C	16	82	490	0.63	0.65	0.68	0.03
S29	29	95	360	0.30	0.12	0.48	none
S29/A	23	80	380	0.27	0.13	0.54	0.03
S29/B	24	90	360	0.30	0.27	0.57	0.05
S29/C	26	90	410	0.42	0.34	0.55	0.01
S29/D	22	80	350	0.49	0.82	0.68	0.02

a) Determined by ICP-OES, error ±1. b) From X-ray diffraction patterns relative to amorphous scattering. c) From N_2 physisorption. d) From ^{1}H MAS NMR after subtracting BAS density. e) From ^{1}H MAS NMR after NH_3 adsorption, accuracy ±5%. f) Determined by ^{31}P MAS NMR after TPP adsorption. g) BAS inaccessible for NH_3, determined by ^{1}H MAS NMR.

decreasing Si/Al ratio for S29-derived samples, as it is observed for ZSM-5 desilication performed using parents with an initial Si/Al ratio of 25 or above[18b,23] or 19.[19] X-ray powder diffraction patterns are shown in Figure S1 in the SI. Found reflexes are typical for an MFI crystal structure and similar patterns can be found in literature.[12e,g, h, 24] Note that the crystallinity of the ZSM-5 catalysts is decreasing by up to 20% after desilication. This agrees with expectations from literature,[12c] whereby we note the largely maintained crystallinity of 80% and more indicates a largely maintained MFI crystal structure of our samples. Note that there is no correlation between crystallinity and indicators of desilication strength (for example, a decreasing sample yield in case of low crystallinity or a dependence of the amount of introduced mesopore volume in Table 1). SEM pictures of parents and samples after desilication are found in Figure 1 and show typical small crystallites typical for industrial material. Within the resolution, the shape and dimension of these particles remain also after desilication similar to the parents, as far as one can tell from the SEM pictures. If larger and more regular crystallites are applied, such a partial

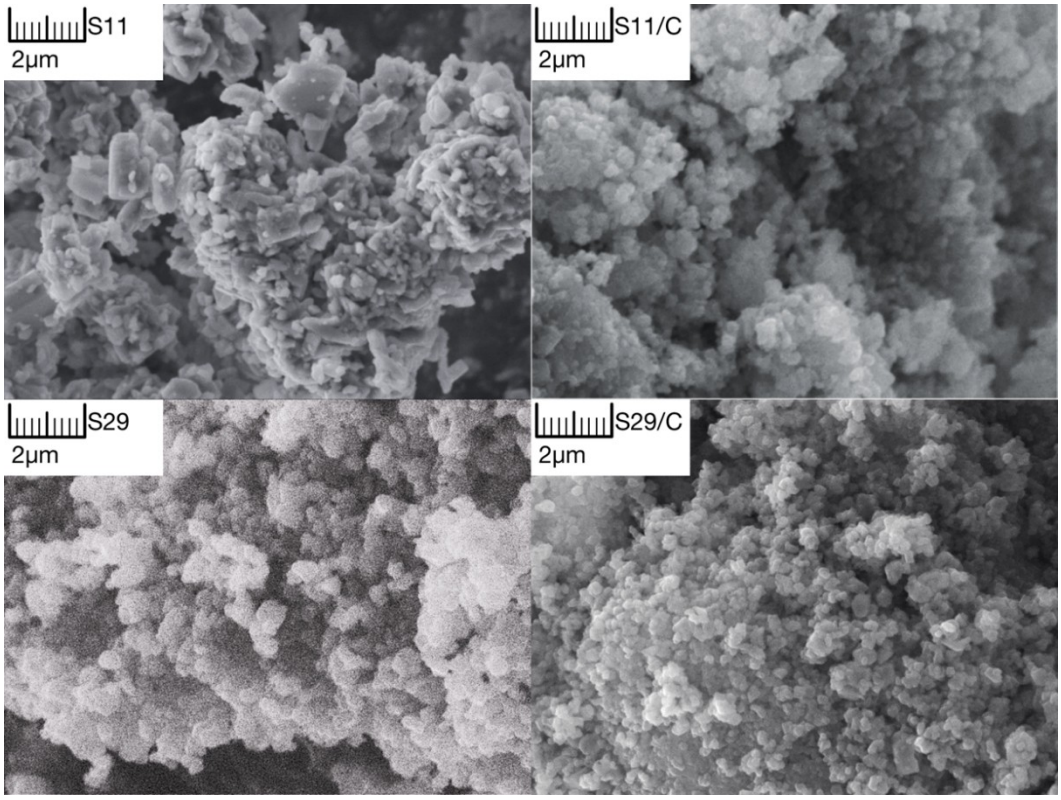

Figure 1. SEM images of parent (S11, S29) and desilicated (S11/C, S29/C) ZSM-5 catalysts.

© 2023 The Authors. ChemCatChem published by Wiley-VCH GmbH

dissolution leads to an obviously visible, roughened surface of larger scale particles if large and homogeneous ZSM-5 crystallites are present.[12b,c] This is not the case for industrially synthesized samples and the shown desilicated ZSM-5 maintain their state of agglomeration and their crystallite shapes.[9]

N_2-physisorption measurements derived by desilication from S11 show an increased BET surface area from 420 m^2/g for S11 to 570 m^2/g for S11/C (see Table 1 and Figures S2, S3a, and S3b in the SI). This increase in surface area is accompanied by an increased mesopore volume ranging from 0.14 to 0.63 mL/g. Thus, the desilication in aqueous NaOH was successfully applied to introduce mesopores into the samples derived from S11. The samples derived from S29 show also increased BET surface areas from 360 to 410 m^2/g, but no direct correlation between BET surface area and mesopore volume is observed. Sample S29/C has the highest surface area, however, the value is for the other desilicated samples even slightly smaller than the parent's surface area. The mesopore volume of the samples increases stepwise from parent to sample S29/D, from 0.27 to 0.49 mL/g, respectively. Note that S29/D was generated by the use of potassium hydroxide (KOH) while other desilication parameters stayed similar. This was done, as it was in a previous study on ZSM-22 zeolites shown that the desilication agent KOH yields under similar conditions more mesopores than NaOH.[12f] Also for the herein used ZSM-5 the use of KOH improved the desilication efficiency (see Experimental Section). We conclude that mesopores were successfully introduced in the S29 parent, however, the desilication efficiency was far lower than for the S11-derived samples but could be increased using KOH instead of NaOH. Comparing with literature findings, we expected the opposite as the lower Si/Al ratio should prevent a fast dissolution and a Si/Al ratio range from 25 to 50 was formerly identified as most promising for effective desilication.[12e] However, in this respect it is worth noting that herein the BET surface area increased to a higher extent than the mesopore volume, which could be increased from 0.30 to 0.32 mL/g only. The differences to literature are thus caused by the different parents applied in our work. This agrees with literature, as it is known that morphology and defects present in the parent significantly affect the desilication of ZSM-5 samples and change properties of derived samples.[12b,19] This clarifies that it is necessary to optimize the desilication procedure individually for each catalyst parent.

The chemical nature of aluminum before and after desilication is another important and after post-modification frequently changing property. It is usually differentiated between aluminum in tetrahedral coordination, that gives rise to BAS in form of bridging Si(OH)Al groups, and aluminum in pentahedral or octahedral coordination, mainly in form of extra-framework species, that could have been deposited within the pores of ZSM-5 zeolites during desilication and cause presence of Lewis acid sites (LAS).[12c,12f,14] ^{27}Al MAS NMR spectra of all samples were recorded in hydrated state of the samples and are found in Figure S4 in the SI. Therein, in accordance with literature, peaks at $\delta_{27Al} = 54$ ppm are attributed to aluminum in tetrahedral coordination that is located within the zeolite framework, whereas peaks around ~0 ppm are attributed to aluminum in octahedral coordination and thus extra-framework position.[11a,25] Clearly the spectra of parents and desilicated samples are almost identical and show only a negligible amount of extra-framework aluminum. This furthermore indicates that the proportions between framework and extra-framework aluminum were maintained. Remarkably, parent S11 and sample S11/A show an asymmetric central peak and weak intensity in the range of 40 to 30 ppm. This usually indicates that also disturbed tetrahedral or pentahedral coordinated aluminum is present in the material.[26] Thus, as some aluminum in unfortunate location is removed from the distribution of chemical shifts in the central peak and compared to the other samples, the chemical shift of the main peak of S11 changes slightly downfield to about ~55 ppm. However, as peaks at −1 ppm remain similarly weak, there was no additional deposition or removal of extra-framework aluminum upon desilication. Thus a successful introduction of mesopores by desilication was verified. Next, the properties of BAS are investigated.

Investigations on BAS and surface hydroxyls

First the nature of present surface hydroxyls shall be discussed. Si(OH) associated with ZSM-5 crystal defects lead to a faster deactivation in the conversion of methanol.[18a] Reason therefore might be the strong affinity of polar molecules like alcohols to Si(OH)-rich defects.[27] The Si(OH) density of our samples calculated from quantitative ^{1}H MAS NMR is given in Table 1. As the external surface area is approximately constant, monitored changes in Si(OH) density upon desilication arise primarily from dissolution of the framework, which usually introduces defects. While the Si(OH) densities of softly desilicated S11/A and S29/A remain close to the densities of the parent samples, all harsher desilicated samples have increased Si(OH) density. This is reasonable, as the necessarily introduced additional surface area is partially saturated with Si(OH) groups. Thus, the harsher the desilication we apply the larger the amounts of defects introduced and the more Si(OH) are necessary to terminate the ZSM-5 crystallite surface.

The total Brønsted acid site (BAS) density of the samples was determined by loading the samples with the probe molecule NH_3. Contact with BAS results in the formation of ammonium ions that are accurately quantifiable via ^{1}H MAS NMR spectroscopy (see Figure S5 in the SI).[28] As discussed previously, the parent S11 contains BAS sites inaccessible by NH_3 as result of blocked pores.[9] This is evidenced by the peak at $\delta_{1H} = 3.9$ ppm assigned to uncovered BAS. Thus some BAS persist the loading and did thus not react to ammonium ions. Conversely, the ^{1}H MAS NMR spectra of sample S11/A after NH_3-loading show a BAS density of 1.00 mmol/g, which corresponds to almost quantitative BAS accessibility (with 1.04 mmol/g maximum BAS density for a Si/Al ratio of 15). Also on samples S11/B and S11/C all BAS were accessible for NH_3, but the harsher desilication also decreased the BAS density. This means the weaker desilication lead to a better accessibility of BAS for S11-derived samples, maybe by removing selectively amor-

© 2023 The Authors. ChemCatChem published by Wiley-VCH GmbH

phous deposits in the samples, whereas harsher conditions lead to a much faster, and thus less selective, desilication of the ZSM-5 framework. This agrees with literature, where comparable variations between Si/Al ratio and BAS density were reported.[12e,15] In case of S29-derived samples, a slightly increasing BAS density after desilication is found. This is in line with the decreasing Si/Al ratio. Thus, we conclude that the aluminum present in S29-derived samples is also becoming better accessible. In case of S29/D, the BAS density reaches the maximum value expected at this Si/Al ratio, considering the presence of EFAl traces indicated by ^{27}Al MAS NMR spectra. Again, in previous investigations different trends regarding the change in BAS density were revealed, but most frequently a decreasing BAS density of ZSM-5 after desilication was reported.[11e,12b,e,g,h,15,19] These discrepancies could emerge from the presence of inaccessible BAS in some cases, as herein demonstrated in case of parent S11. In other words, a partial loss in BAS density is to a certain extent compensated, if formerly inaccessible BAS become accessible due to mesopore formation and removal of deposits.

The herein observed changes in BAS density can be further rationalized with respect to zeolites with other structures: An increase in BAS density upon desilication, due to a better accessibility of BAS, was found for 10-/8-membered ring zeolite SUZ-4. This zeolite structure contains largely inaccessible 8-membered ring pores so small that they even prevent efficient ion exchange of potassium counter ions. However, some of these BAS were made accessible by desilication.[11c] In contrast, for the 10-membered ring zeolite ZSM-22 a decreased BAS density was found upon desilication, because all BAS were already initially fully accessible.[12f] Thus there was no threshold to compensate for, upon desilication, lost BAS. For the herein discussed ZSM-5 samples, we note that for both parents S11 and S29 the measured BAS density is far lower (0.66 + 0.22 and 0.48 mmol/g) then expected solely from the Si/Al ratio (1.39 and 0.56 mmol/g). This lower accessibility is frequently observed for industrially synthesized material. For example, mordenites with Si/Al = 7 and 11 had instead of the expected 2.1 and 1.4 mmol/g only 2.0 and 1.1 mmol/g detectable BAS density, respectively.[29] Thus in case of S11 the amount of BAS increases first comparing S11 and S11/A, before harsher desilication leads to a decreased BAS density for S11/B and S11/C. In case of S29-derived samples, the desilication dissolved more silicon, presumably in silicon-rich domains, which lead to the decreased Si/Al ratio and the increased BAS density. Obviously, the amount of blocked BAS before desilication determines if the desilication leads to an increased (if large amounts of BAS become accessible as result of the treatment) or a decreased BAS density (if already the parent catalysts are largely accessible). As the accessibility of ZSM-5 parent BAS is a property strongly determined by the zeolite synthesis procedure, it is no surprise that an acid wash cannot completely out rule changes in acidity in one or another direction.

The location of BAS and its impact on the conversion of alcohols was addressed previously.[11f,19] After desilication, BAS formerly located inside ZSM-5 micropores might get exposed to mesopores or to the external surface. Such BAS might be of great relevance for alcohol conversion reactions, since the location of BAS within the micropore system induces the shape-selectivity as key parameter for receiving the desired product.[4,30] In order to distinguish between BAS on the external surface, those in mesopores, and those in micropores, we apply a method that combines the probe molecules ammonia and triphenylphosphine (TPP).[31] ^{31}P MAS NMR spectra applying the probe molecule TPP are found in Figure 2. While ammonia is small and able to enter all accessible pores (*vide supra*), the TPP molecule diameter prevents it from entering the 10-membered ring pores of ZSM-5 zeolites (calculated TPP diameter 1.08 nm[32]). In other words, the protonation of TPP in strict 1:1 stoichiometry after loading, indicated by a broad peak at δ_{31P} = ~7 ppm in ^{31}P MAS NMR spectra, can only occur if some BAS are not located in the shape-selective MFI micropore system (see Table 1 for the amount of accessible BAS). These unselective BAS must thus be located within introduced mesopores or on the external surface of the crystallite. Physisorbed TPP is found at a chemical shift of $\delta_{31P} \approx -6$ ppm and proves an excess of the probe molecule applied to ensure a quantitative detection of accessible BAS.[31] In case of the parents S11 and S29 no protonation of TPP was evidenced and thus no external BAS are present (see Figure 2).[9] However, for S11-derived samples we find up to 0.03 mmol/g unselective BAS after desilication. For S29-derived samples, the trend is less obvious. Whereas the unselective BAS density increases from S29 to S29/B to up to 0.05 mmol/g, we find a drop for the samples S29/C and S29/D to 0.01 respectively 0.02 mmol/g. Again, the harshness of desilication leads to a rather unselective framework dissolution and in result fewer unselective BAS. We conclude that the amount of external BAS density that is generated is generally low, however, is not strictly correlated with desilication strength or introduced mesopore volume. Similar amounts of unselective BAS in the range 1 to 13 mmol/g were determined by IR measurements after collidine loading on desilicated ZSM-5

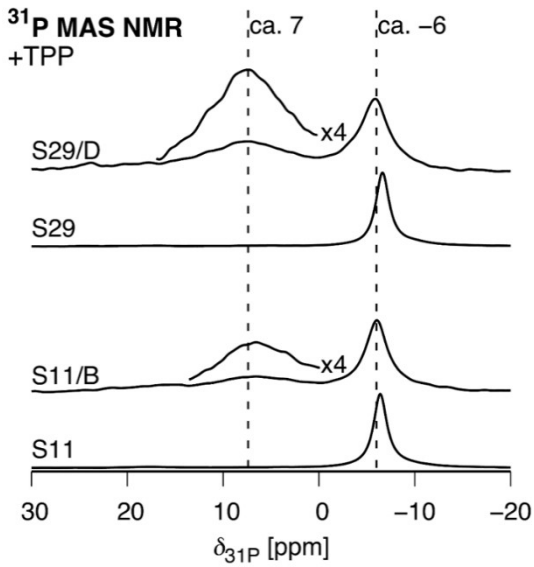

Figure 2. ^{31}P MAS NMR spectra after loading TPP on the parents and desilicated materials.

© 2023 The Authors. ChemCatChem published by Wiley-VCH GmbH

catalysts.[19] Thus, like the total BAS density also the amount of unselective BAS inside mesopores must be determined individually on each sample after desilication.

Finally, we investigate the strength of the BAS present on our parent and desilicated samples. A typical way to determine this parameter is the loading of samples with the probe molecule acetonitrile-d_3 in combination with ^{1}H MAS NMR spectroscopy.[33] The strength of zeolite BAS is then characterized by the adsorption-induced chemical shift, $\Delta\delta_{1H}$, of BAS protons before and after loading.[34] The ^{1}H MAS NMR spectra of our parents and of desilicated samples are found in Figure 3. Upon loading acetonitrile-d_3, we find that the peak of BAS formerly located at $\delta_{1H}=3.9$ ppm is significantly shifted, as the adsorbed base leads to de-shielding of the acidic proton. The strength of this interaction is represented by $\Delta\delta_{1H}$ which is found to be 7.1 ppm for both parents and desilicated samples. This is a typical $\Delta\delta_{1H}$ value frequently measured for other ZSM-5 zeolites.[10c,11c,24] Also in case of desilicated ZSM-22 the acid site strength of BAS was not affected by desilication.[12f] For comparison, BAS in zeolite H–Y with Si/Al ratio of 2.7, and Al(OH) groups in MOF MIL-53 show a significantly lower $\Delta\delta_{1H}$ of 3.0,[35] 5.1,[36] and 1.2 ppm,[37] respectively. It is generally accepted that a maintained adsorption-induced chemical shift $\Delta\delta_{1H}$ indicates a maintained BAS strength for desilicated ZSM-5.[34] Thus, the BAS strength was maintained upon desilication of ZSM-5 zeolites.

Performance in the ethanol-to-aromatics conversion (ETA)

After elucidating the ZSM-5 material properties the effect of ZSM-5 desilication on the ethanol-to-aromatics conversion (ETA) was evaluated. There is no subsequent dealumination of the samples but a detailed discussion of dealuminated ZSM-5 applied in ethanol conversion, also in combination with steaming and desilication, is found elsewhere.[11e] All plots of catalytic measurements and ETA product distribution (product yields at 100% ethanol conversion, considering ethylene a product and ignoring loss due to coke) of the effluent are found in Figures S6 to S12 and Table S1 in the SI, while further data on the catalytic behavior of the parents in ETA is found elsewhere.[9] We first compare how desilication affects the product distribution obtained during ethanol conversion over desilicated samples derived from two different parents, S11 and S29 individually. For the family based on S11 we find rather similar selectivity to relevant products as depicted in Figure 4. When it comes to BTEX aromatics, desilication of the S11 parent has a negative effect as the BTEX selectivity decreases from 35.9 to 31.5%. Likewise, the yield of paraffins drops in case of harsh desilication. This agrees with literature where a similar drop in aromatic yield (~factor 2) was observed for nanosized ZSM-5 parent after desilication.[19] Obviously, desilication and better transport leads to a better diffusion of C_4 Olefins, C_5, and C_{6+} fractions out of the pores. This prevents a subsequent cyclization and aromatization to form BTEX aromatics. Thus we can support literature results concluding that a complex interplay between transport and reaction properties determine the effluent composition after desilication.[11f] Note the small

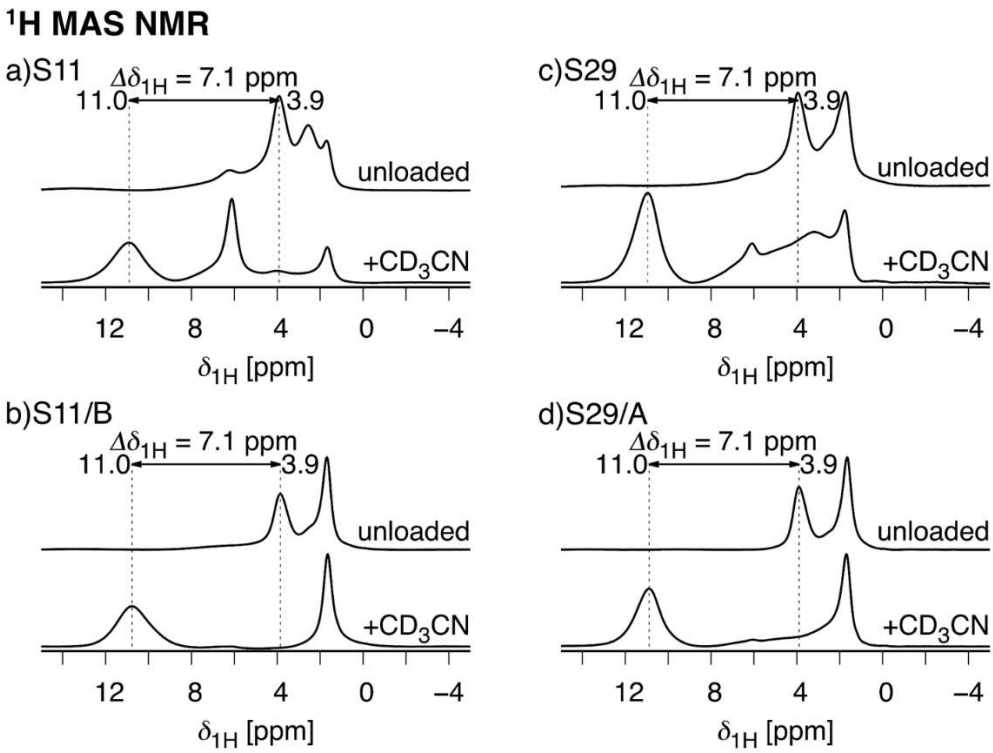

Figure 3. ^{1}H MAS NMR spectra before and after acetonitrile-d_3 loadings on a) parent S11, b) desilicated S11/B, c) parent S29 and d) desilicated S29/A.

© 2023 The Authors. ChemCatChem published by Wiley-VCH GmbH

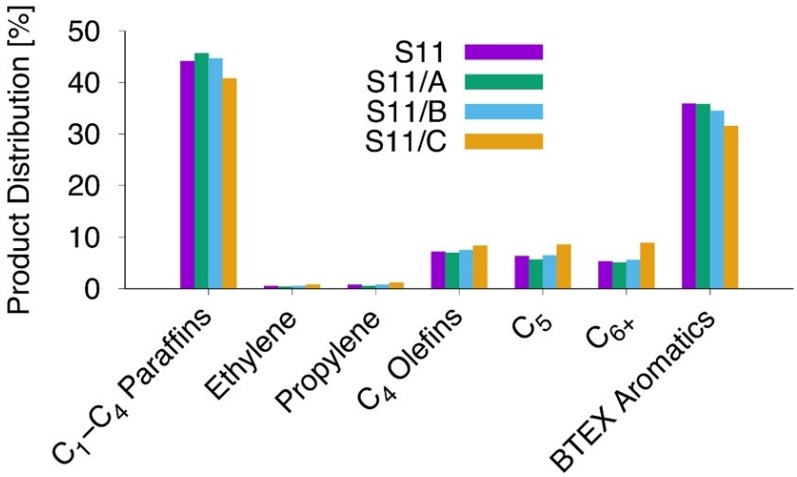

Figure 4. Effect of desilication on the ETA product distributions over S11-derived samples at WHSV = 1.0 h^{-1}, T = 673 K, p(ethanol) = 0.3 bar, flow = 15 mL/min.

amounts of ethylene, a product generated through direct dehydration of ethanol,[7] and propylene, generated after cracking of larger olefins.[8] All in all, despite significantly increased mesopore volume and maintaining the high BAS density, desilication of S11 parent did not lead to more BTEX aromatics in the ETA conversion.

We next investigate the product distributions of S29-derived samples shown in Figure 5. Here an increased amount of BTEX aromatics is found, raising from 30.2 to 32.4%. However, this is accompanied by an increasing amount of paraffins that raises from 34.9 to 40% (which is still smaller than in case of any S11-derived samples that were discussed previously). Also in contrast to the S11-derived samples, we find with increasing desilication strength a decreasing amount of C_4 Olefins, C_5, and C_{6+} fractions in the product distribution. The quantities of ethylene and propylene are, in case of S29-derived samples, by a factor of 3 to 4 higher than for the S11-derived samples. Ethylene and propylene quantities decrease slightly with increasing desilication strength. Thus, whereas in case of the S11-derived samples very high paraffin yields are observed, for S29-derived samples we find larger amounts of other products like BTEX aromatics, olefins and large-chain products. Thus, when parents with for desilication suited properties are used, the desilicated samples derived from them can indeed have a beneficial impact on the BTEX yield of the ETA conversion.

In a next step, we will discuss the lifetime and deactivation of ZSM-5 catalysts applied in the ETA conversion before and after desilication. The lifetimes, conversion capacities, and coke amounts (calculated on the mass of ZSM-5 catalysts) were extracted and tabulated in Table 2. Obviously, the desilication of microporous parents lead always to strongly enhanced (factor ~4 and above) lifetimes in the ETA conversion. In line with this enhanced lifetime, the catalysts show a higher conversion capacity. For comparison, another microporous ZSM-5 shows 100.0 g/g conversion capacity (this value was derived from the reported deactivation at WHSV = 3 h^{-1}), as result of the lower BAS density of 0.34 mmol/g (Si/Al = 43).[9] This agrees with previous findings from literature on ETA conversion over ZSM-5.[19] For S11-derived samples we find a maximum lifetime (and conversion capacity) for S11/B, whereas

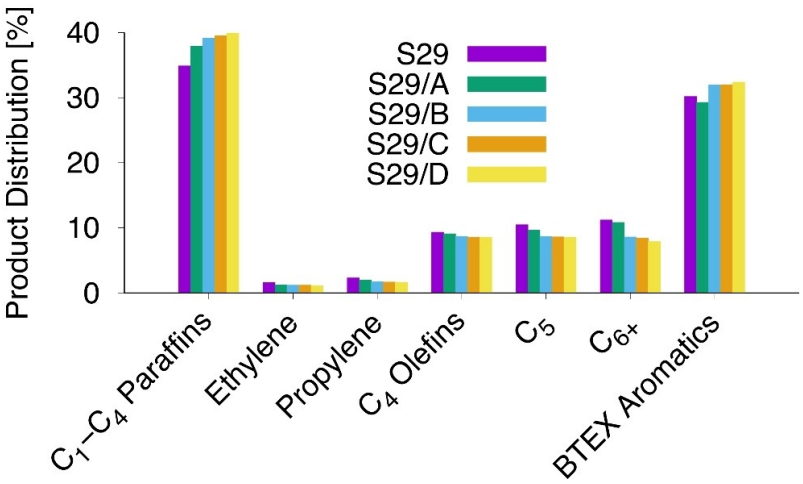

Figure 5. Effect of desilication on the ETA product distributions of S29-derived samples at WHSV = 1.0 h^{-1}, T = 673 K, p(ethanol) = 0.3 bar, flow = 15 mL/min.

© 2023 The Authors. ChemCatChem published by Wiley-VCH GmbH

Table 2. Data on lifetime/deactivation and coking of parents and desilicated ZSM-5.

Material	Lifetime [h][a)]	Conversion capacity [g/g][b)]	Coke [%][c)]
S11	7.5	13.8	12.1
S11/A	29.1	64.9	8.2
S11/B	40.5	82.1	14.1
S11/C	33.0	64.1	12.7
S29	11.4	32.7	7.0
S29/A	79.5	160.5	16.1
S29/B	61.8	136.2	15.9
S29/C	60.7	122.0	17.4
S29/D	47.9	93.9	13.9

a) From catalytic testing; >80% ethylene yield. b) At WHSV = 3 h^{-1}. c) Determined by TGA.

for S29-derived samples the lifetime subsequently decreases if a harsher desilication is applied. In literature, often maximum lifetimes at intermediate desilication are reported for the conversion of methanol.[11d,12f,h] The amount of coke retained within the pores of ZSM-5 catalysts increases, if the catalysts were post-modified by desilication. When desilicated ZSM-5 samples are applied, the different reaction zones of the catalyst bed cannot be distinguished any more as expected from the "burning cigar" model that was introduced for purely microporous materials.[38] This agrees with findings from methanol conversion on desilicated samples, where likewise the different reaction zones became indistinguishable because coke was more homogeneously distributed along the desilicated crystallite.[12f,i] Generally, the feed loss due to coke formation, with respect to the total lifetime, strongly decreases if desilicated samples are applied. Thus, the desilication can also for the ETA conversion strongly boost the lifetime, as result of more pore entrances and mesopores that prevent a fast blocking of pores by coke.

Finally, we wanted to identify property-performance relations for the performance parameters BTEX yield (Y_{BTEX}), lifetime, and coke formation. General trends are best identified by correlation between single parameters (see Figure 6). For example, the total BAS densities of ZSM-5 catalysts determine

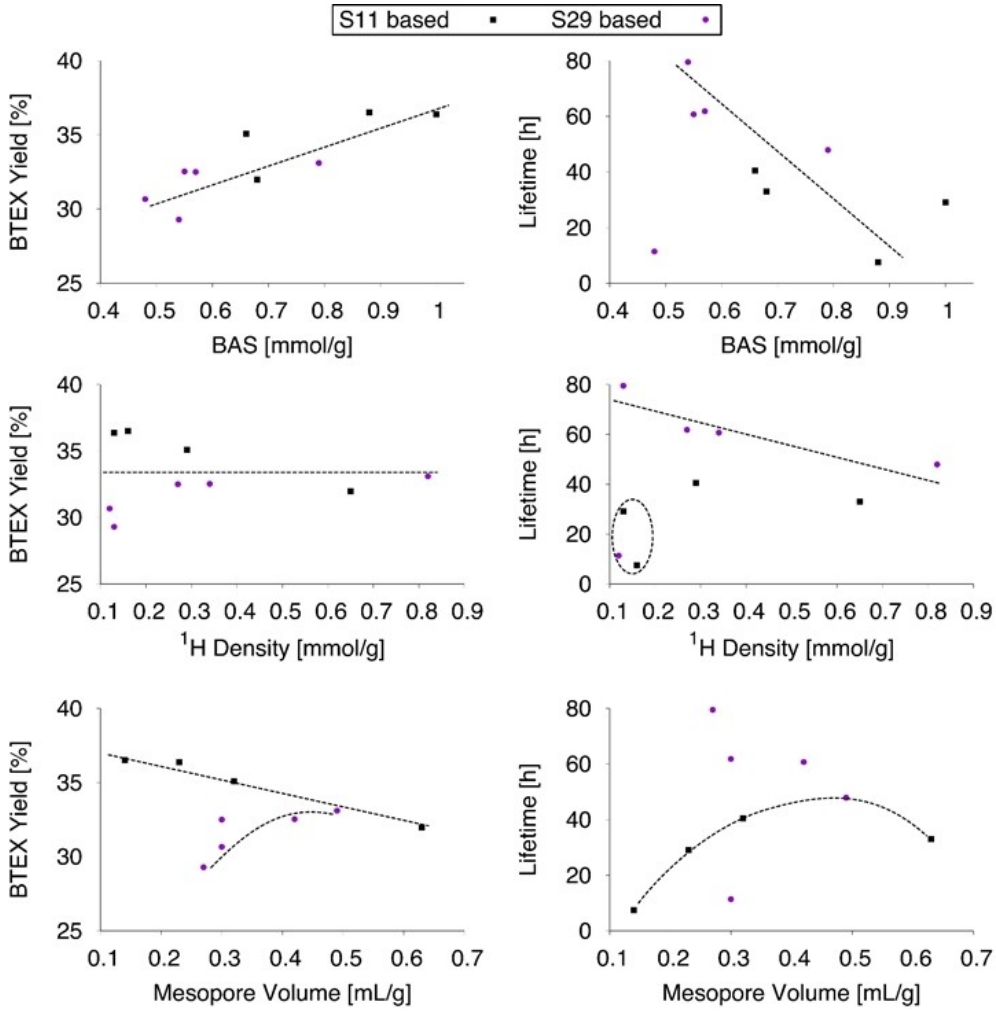

Figure 6. Correlation between material properties and ETA performance for parent and desilicated ZSM-5 zeolites with trendlines to guide the eye. BTEX yield defined at 100% ethanol conversion considering ethylene a product.

© 2023 The Authors. ChemCatChem published by Wiley-VCH GmbH

the product yields in methanol-to-olefin conversion.[10c,24,39] If not all BAS are accessible, like for parent S11, this can be rationalized as fewer catalyst mass available.[40] We correlated the BTEX selectivity of our catalysts in ETA conversion against the total BAS density of our materials. The BTEX yields are located between 29 and 36% and an increase in BTEX yield with increasing BAS density is observed. This is in line with findings on the impact of BAS density derived from purely microporous ZSM-5 catalysts.[9,41] With increasing BAS density we observe also a decreased lifetime of our catalysts. This is caused by the increased amount of aromatics formed that lead to deactivation and was already described for microporous ZSM-5 catalysts.[9,11e] In desilicated samples, however, this effect is overshadowed by a longer lifetime as result of better transport properties.[11f] We thus conclude that the general trends regarding BAS density are prevailed. And while increased BAS density is beneficial for increased BTEX formation, it decreases the lifetime.[9,41] However, desilication also changes the acid properties of catalysts. Thus, the total BTEX yield generated over desilicated ZSM-5 catalysts is a balance between the effects from introduced mesoporosity and changed BAS density.

Si(OH) groups might influence the coking of ZSM-5 catalysts and in Figure 6 it is thus visualized how their density correlates with BTEX yields or lifetimes of catalysts. We evidence that Si(OH) groups are not leading to more BTEX aromatics on all samples and conversely, at low Si(OH) density, about 5% more BTEX yield is found. However, at increasing Si(OH) density these differences even out and about the same BTEX yields are generated. For desilicated samples also a slight decrease in lifetime is observed, proportional to the Si(OH) group density. The parents S11 and S29 naturally show few Si(OH) groups and a shorter lifetime, mainly due to absence of mesoporosity. An outstandingly short lifetime is also monitored for catalyst S11/A as result of its high BAS density (*vide supra*). Summarizing, if more than 0.3 mmol/g Si(OH) groups are present, no impact on the BTEX yield in the ETA effluent is observed. In tendency a decreased lifetime for desilicated ZSM-5 catalysts is caused by the increasing Si(OH) density. Similar reports exist for ZSM-5 catalysts in methanol conversion.[18] Thus also for the ETA conversion high Si(OH) densities after desilication should be avoided for maximizing the lifetime.

For the S11-derived samples we find a slightly decreasing BTEX yield in the effluent flow with increasing mesopore volume (see Figure 6). A high BAS density and proximity causes for S11 a high yield of BTEX aromatics (*vide supra*). For S29-derived samples of lower BAS density, the BTEX yield increases with increasing mesopore volume, in agreement with literature on ETA[23] and methanol-to-olefin[18b] conversion. In both literature cases ZSM-5 with higher Si/Al ratio were applied and thus S29-derived samples are closer to the findings reported therein. Lifetime with respect to introduced mesopore volume first increases, before a plateau is reached for S11-derived samples. Thus few mesopores are able to increase the lifetime significantly, while very high mesopore volumes (and mass loss) are not necessary. For S29, there is barely a correlation between lifetime and mesopore volume, while in total (see Table 2) the desilication leads to an increased ETA lifetime. Conclusively, an increased mesopore volume is beneficial for longer lifetimes especially for a lower Si/Al ratio of 11 (parent), while BTEX yields are determined by the BAS density of catalysts.

We summarize that a large variety of catalyst properties is changed upon desilication. How a property changes is determined by the properties of the utilized ZSM-5 parent. Due to better transport properties in desilicated samples, the lifetimes in ETA conversion are often increased. A high Si(OH) density can to some extent lead to faster coking and deactivation of samples. Desilication and mesoporosity *per se* do not lead to an increase in BTEX aromatics. The BTEX product yields are determined by interplay of BAS density, responsible for the maximum amount generated, and transport properties, responsible with the fraction of aromatics that leave the pores before coke is formed. The impact of desilication on catalyst lifetimes is comparable for both alcohol feeds, methanol and ethanol. Despite desilication cannot be used to enhance the selectivity to BTEX aromatics significantly, larger lifetimes are achieved at rather soft desilication. This makes desilication a promising tool to enhance the lifetime by a simple post-modification procedure.

Conclusions

We successfully introduced mesopores into ZSM-5 parents by using desilication. The crystallinity of all desilicated samples decreased slightly compared to the parents. Introduction of mesopores resulted in increased BET surface areas and the stronger the applied desilication, reflected by a lower yield of sample after NaOH-treatment, the higher the introduced mesopore volume. A parent with Si/Al ratio of 11 yielded samples with higher mesopore volume than a parent with a Si/Al ratio of 29. The desilication efficiency of ZSM-5 zeolites, the amount of mesopores generated per mass loss, could be improved by using KOH instead of NaOH as desilication agent. We conclude that not only the Si/Al ratio but also the morphological properties of the parents determine the properties of the derived desilicated samples. Comparable states of aluminum within the pores of likewise S11- and S29-derived samples were verified. Desilication increased the Si(OH) density of all samples significantly. A strong discrepancy between theoretically expected and indeed accessible Brønsted acid sites (BAS) is noted. A large amount of inaccessible sites in the parent can compensate for a reduced BAS density as result of the desilication. We measured the amount of unselective BAS located in mesopores utilizing the probe molecule triphenylphosphine in combination with quantitative ^{31}P MAS NMR spectroscopy. While no BAS in mesopores were found for the parents, all desilicated samples contained minor amounts of BAS in mesopores (0.01 to 0.05 mmol/g). The BAS strength of desilicated samples remained comparable to the strength of the parents.

We find that an increase in BAS density leads, as in microporous ZSM-5, to a higher extent of benzene, toluene, ethylbenzene, and xylene (BTEX) aromatics formed. On the

© 2023 The Authors. ChemCatChem published by Wiley-VCH GmbH

same hand, the increased BAS density also decreases the lifetime. Catalytic studies revealed also a decrease in BTEX yield for S11-derived samples when increasing the mesopore volume too much. An increased yield of BTEX, with increasing desilication strength, is observed for S29-derived samples. Lifetimes in general strongly increase upon desilication by a factor of about 4 for both catalyst families, whereas coke amounts of deactivated samples increase only slightly. Thus fewer ethanol is lost as coke in desilicated samples. The Si(OH) groups introduced upon desilication did not alter the BTEX yield, however, they decreased the lifetime and should thus be avoided. The effect of introduced mesopore volume on BTEX yields depended on the Si/Al ratio of the applied parent, slightly decreasing for S11-derived samples and increasing for S29-derived samples. We conclude that BTEX yields barely change by introducing mesopores by desilication.

In this study, we separate effects from mesopore introduction from those resulting from desilication. In particular the effect of changed BAS and Si(OH) group density on the catalytic performance and lifetime of ZSM-5 zeolites in ethanol-to-aromatic (ETA) conversion. The BTEX yield is to large extent predetermined by the BAS density and not or only scarcely improved when comparing to purely microporous samples. On the other hand, desilication is a prominent tool to increase the lifetime of ZSM-5 catalysts applied in the ETA conversion and to reduce feed loss due to coking. This effect is fortunately already obvious for low desilication strength and thus large loss in ZSM-5 catalyst material can be avoided.

Experimental

Material preparation

The industrially synthesized H-ZSM-5 zeolites CBV 2314 and CBV 5524G were purchased from Zeolyst Inc., USA. Prior to use they were calcined (6.5 h at 813 K in synthetic air) and afterwards transformed into their stabilized ammonium form by ion exchange with ammonium nitrate (Merck, Germany). Briefly, 1 g of the ZSM-5 material was reacted in 10 mL of a 0.1 M ammonium nitrate solution at 353 K for 3 h. After that, the exchanged material was filtered off and washed with demineralized water until nitrate free, followed by a drying process at 373 K for 16 h. This process yielded the two parent zeolites (S11 and S29) and the parents for the subsequent desilication. For a typical desilication 4 g of the ammonium exchanged parent was added to 120 mL aqueous sodium or potassium hydroxide at the reaction temperature of 338 K and stirred for a certain time. Details on treatments and yields are given in Table 3. Note that the samples were named after the yield received, with letters A to D representing a decreasing yield and thus increasingly harsh desilication of the parent. The "desilication efficiency" is the amount of mesopore volume per catalyst mass that was generated per % lost parent ZSM-5 mass (defined as 100 – Yield% after desilication from Table 3).

After completion, the reaction was quenched in an ice bath and the aqueous solution immediately removed using centrifugation (5000 rpm, 10 min). The received solid was then two times washed with demineralized water. To remove formed extra-framework aluminum deposits and exchange counter ions, a subsequent treatment with aqueous acid was performed.[12e,f,15] Therefore the dried material (373 K, 16 h) was added to calculated amounts (100 mL/g) of a 0.5 M aqueous hydrochloric acid solution and treated for 6 h at 338 K. The reaction was again quenched using an ice bath and the solution was removed via centrifugation (5000 rpm, 10 min). The solid residue was then washed in demineralized water. A complete ion exchange was verified by ICP-OES. Samples were named after their parent (S11 or S29) and decreasing desilication strength/increasing catalyst yield symbolized by alphabetically ordering the samples (A, B, C, D).

Characterization

Inductively coupled plasma optical emission spectrometry (ICP-OES) was used to determine the chemical composition utilizing an IRIS Advantage instrument. The structure of the zeolite samples under study was investigated by X-ray diffraction (XRD). Therefore, a Bruker D8 diffractometer equipped with an X-ray tube for CuKα radiation ($\lambda = 1.5418$ Å) was used. The XRD patterns were recorded in a 2Θ range of 4–50° for the zeolite samples. The crystallinity of the samples was determined comparing the diffraction pattern intensity before and after subtracting the amorphous scattering using the Bruker software EVA. For the investigation of the pore structure and volumes, nitrogen physisorption was performed at 77 K using a Quantachrome Autosorb 3B. Prior to measurements, the samples were activated at 623 K for 16 h. The surface of materials was evaluated using the Brunauer-Emmett-Teller (BET) equation. The micropore volume was determined according to the *V-t* method (de Boer) and the mesopore volume was determined as difference to the total pore volume of $p/p_0 = 0.99$.

^{1}H, ^{27}Al, and ^{31}P MAS NMR spectroscopy was performed on a Bruker Avance III 400 WB spectrometer with a magnetic field of 9.4 T. The resonance frequencies were 400.1 MHz (^{1}H), 104.2 MHz (^{27}Al), and 161.9 MHz (^{31}P). Quantitative ^{1}H and ^{31}P measurements were performed after $\pi/2$ excitation, whereas for qualitative ^{27}Al $\pi/8$

Table 3. Treatment conditions for synthesis of mesoporous ZSM-5.

Sample	Base treatment	Acid treatment	Yield from parent [%]	Desilication efficiency [μl/g][a)]
S11/A	0.4 M NaOH 30 min	0.5 M HCl 6 h	80.2	4.5
S11/B	0.8 M NaOH 30 min	0.5 M HCl 6 h	61.3	4.7
S11/C	1.0 M NaOH 30 min	0.5 M HCl 6 h	45.5	9.0
S29/A	0.2 M NaOH 15 min	0.5 M HCl 6 h	74.3	0
S29/B	0.4 M NaOH 15 min	0.5 M HCl 6 h	48.1	0
S29/C	0.4 M NaOH 30 min	0.5 M HCl 6 h	38.8	0.3
S29/D	0.4 M KOH 30 min	0.5 M HCl 6 h	32.0	2.8

a) Defined as mesopore volume generated per lost ZSM-5 mass (100–Yield%)

© 2023 The Authors. ChemCatChem published by Wiley-VCH GmbH

excitation was used. Activation of the samples before ^{1}H and ^{31}P MAS NMR measurements was executed using the following temperature program: 723 K for 12 h at $p < 10^{-2}$ mbar with a heating rate 1 K/min. The samples for the ^{27}Al MAS NMR measurements were in a fully hydrated state. 4 mm rotor spinning rates of 8 kHz (^{1}H, ^{27}Al) and 10 kHz (^{31}P) were applied and the repetition times between scans were 20 s (^{1}H, ^{31}P) and 0.5 s (^{27}Al). ^{31}P MAS NMR measurements were recorded using high-power proton decoupling (HPDEC). For a determination of the BAS density, ammonia loading with 60 mbar ammonia gas (Westfalen, Germany) was performed through a vacuum line. To desorb excess ammonia, a subsequent evacuation at 453 K for 2 h was performed. For quantification of ^{1}H MAS NMR spectra a dehydrated zeolite H,Na-Y (35% ammonium exchanged) was used as an external standard. Triphenylphosphine (TPP) loadings were performed using a glove box purged with N_2.[31] Briefly, dehydrated sample material was mixed with calculated amounts of solid TPP (1 to 10 mg) and dry dichloromethane (DCM) (0.8 to 1 mL) was added for its dissolution in the N_2-purged glove box for 1 h. After equilibration the sample was placed in a desiccator purged with N_2 for at least 2 days to remove the DCM solvent completely. For quantification, hydrated zeolite VPI-5 was used as an external standard, as described elsewhere.[12f,32] The evaluation of the NMR spectra was performed using TopSpin and Dmfit.[42]

Catalytic testing

The materials were pressed and sieved into a particle size distribution between 200 and 315 μm. The catalytic tests of the materials were performed in a 7 mm diameter fixed bed reactor under optimized conditions for BTEX formation ($p_{Ethanol} = 0.3$ bar, $T = 673$ K) determined previously.[9] The WHSV was set using different amounts of catalysts material. To suppress the effect of the residence time, the catalyst materials were diluted with inert sea sand (Grüssing, Germany) to ensure that the catalytic bed had the same length (5.3 cm to 5.6 cm). The materials were activated *in situ* using a nitrogen flow of 50 mL/min by applying a heat treatment at 383 K for 1.0 h after temperature increase with a rate of 3 K/min, and a subsequent treatment at 723 K for 0.5 h, with a heating rate of 1.9 K/min. For the reaction a nitrogen flow of 15 mL/min was set through a saturator filled with chromosorb and ethanol (Sigma-Aldrich, Germany and Merck, Germany) that was heated to 326.5 K to set the partial pressure of ethanol ($p_{Ethanol}$) to 0.3 bar. The nitrogen flow saturated with ethanol was then directed into the reactor, whereby all piping after the saturator to the GC inlet was heated at >393 K to prevent product condensation. The GC for analyzing the product stream was a Hewlett Packard series II 5890 equipped with an FID and an Agilent PoraPLOT Q column (52.5 m, 0.32 mm, 10 μm). Missing data was interpolated and indicated by hatched bars (in Figures in the Supporting Information, SI). Catalyst lifetime was defined as time until the ethylene yield in the effluent reaches >80% ethylene. The coke amount in the fully deactivated ZSM-5 catalysts fraction was determined by TGA on a Setaram Setsys 16/18 analyzer. Typically 30 mg material were placed in a flow of synthetic air while increasing the temperature by 10 K/min to 1223 K. The final temperature was maintained for 2 h and the total coke amount calculated based on the mass of pure ZSM-5 zeolite.

Acknowledgements

The authors want to thank Heike Fingerle for ICP-OES measurements, Maximilian Schmidt for SEM measurements, and Ann-Katrin Beurer, Dorothea Häussermann, Faeze Tari, Nagme Ay, and Michael Benz for N_2-Physisorption measurements. Funded by the Deutsche Forschungsgemeinschaft (DFG, German Research Foundation) under Project 471005971. Open Access funding enabled and organized by Projekt DEAL.

Conflict of Interests

There is nothing to declare.

Data Availability Statement

The data that support the findings of this study are available from the corresponding author upon reasonable request.

Keywords: Desilicated zeolite ZSM-5 · ethanol-to-aromatics conversion · biomass conversion · solid-state NMR probe molecules · hierarchical zeolites

[1] N. M. Eagan, M. D. Kumbhalkar, J. S. Buchanan, J. A. Dumesic, G. W. Huber, *Nat. Chem. Rev.* **2019**, *3*, 223–249.
[2] D. Dodds, B. Humphreys, in *Catalytic Process Development for Renewable Materials*, **2013**, pp. 183–237.
[3] a) Q. Bu, H. Lei, A. H. Zacher, L. Wang, S. Ren, J. Liang, Y. Wei, Y. Liu, J. Tang, Q. Zhang, R. Ruan, *Bioresour. Technol.* **2012**, *124*, 470–477; b) J. Zhang, J. Sun, Y. Wang, *Green Chem.* **2020**, *22*, 1072–1098.
[4] M. Stöcker, *Microporous Mesoporous Mater.* **1999**, *29*, 3–48.
[5] P. Tian, Y. Wei, M. Ye, Z. Liu, *ACS Catal.* **2015**, *5*, 1922–1938.
[6] E. G. Derouane, J. B. Nagy, P. Dejaifve, J. H. C. van Hooff, B. P. Spekman, J. C. Védrine, C. Naccache, *J. Catal.* **1978**, *53*, 40–55.
[7] K. Van der Borght, R. Batchu, V. V. Galvita, K. Alexopoulos, M.-F. Reyniers, J. W. Thybaut, G. B. Marin, *Angew. Chem. Int. Ed.* **2016**, *55*, 12817–12821.
[8] A. D. Chowdhury, A. Lucini Paioni, G. T. Whiting, D. Fu, M. Baldus, B. M. Weckhuysen, *Angew. Chem. Int. Ed.* **2019**, *58*, 3908–3912.
[9] D. Dittmann, C. Rieg, Z. Li, E. Kaya, M. Dyballa, *Energy Fuels* **2023**, *37*, 4566–4579.
[10] a) J. Caro, M. Bülow, M. Derewinski, J. Haber, M. Hunger, J. Kärger, H. Pfeifer, W. Storek, B. Zibrowius, *J. Catal.* **1990**, *124*, 367–375; b) D. V. Vu, Y. Hirota, N. Nishiyama, Y. Egashira, K. Ueyama, *J. Jpn. Pet. Inst.* **2010**, *53*, 232–238; c) M. Dyballa, E. Klemm, J. Weitkamp, M. Hunger, *Chem. Ing. Tech.* **2013**, *85*, 1719–1725; d) Z. Zhou, X. Wang, J. Li, Y. Gao, R. Yu, R. Jiang, *Chem. Eur. J.* **2023**, *29*, e202203095; e) J. Huangfu, D. Mao, X. Zhai, Q. Guo, *Appl. Catal. A* **2016**, *520*, 99–104.
[11] a) M. Müller, G. Harvey, R. Prins, *Microporous Mesoporous Mater.* **2000**, *34*, 135–147; b) S. M. T. Almutairi, B. Mezari, E. A. Pidko, P. C. M. M. Magusin, E. J. M. Hensen, *J. Catal.* **2013**, *307*, 194–203; c) M. Dyballa, D. K. Pappas, E. Borfecchia, P. Beato, U. Olsbye, K. P. Lillerud, B. Arstad, S. Svelle, *Microporous Mesoporous Mater.* **2018**, *265*, 112–122; d) Y. Fang, F. Yang, X. He, X. Zhu, *Frontiers of Chemical Science and Engineering* **2019**, *13*, 543–553; e) M. Seifert, M. S. Marschall, T. Gille, C. Jonscher, O. Busse, S. Paasch, E. Brunner, W. Reschetilowski, J. J. Weigand, *ChemCatChem* **2020**, *12*, 6301–6310; f) M. Seifert, M. S. Marschall, T. Gille, C. Jonscher, P. Royla, O. Busse, W. Reschetilowski, J. J. Weigand, *Chem. Asian J.* **2020**, *15*, 3878–3885.
[12] a) T. Weissenberger, A. G. F. Machoke, J. Bauer, R. Dotzel, J. L. Casci, M. Hartmann, W. Schwieger, *ChemCatChem* **2020**, *12*, 2461–2468; b) S. Svelle, L. Sommer, K. Barbera, P. N. R. Vennestrøm, U. Olsbye, K. P. Lillerud, S. Bordiga, Y.-H. Pan, P. Beato, *Catal. Today* **2011**, *168*, 38–47; c) M. Ogura, S.-y. Shinomiya, J. Tateno, Y. Nara, M. Nomura, E. Kikuchi, M. Matsukata, *Appl. Catal. A* **2001**, *219*, 33–43; d) D. Verboekend, A. M. Chabaneix, K. Thomas, J.-P. Gilson, J. Pérez-Ramírez, *CrystEngComm* **2011**, *13*, 3408–3416; e) D. Verboekend, S. Mitchell, M. Milina, J. C. Groen, J. Pérez-Ramírez, *J. Phys. Chem. C* **2011**, *115*, 14193–14203; f) M. Dyballa, U. Obenaus, M. Rosenberger, A. Fischer, H. Jakob, E. Klemm, M. Hunger, *Microporous Mesoporous Mater.* **2016**, *233*, 26–30; g) F. Zhou, Y. Gao, G. Wu, F. Ma, C. Liu, *Microporous Mesoporous Mater.* **2017**, *240*, 96–107; h) C. Mei, P. Wen, Z. Liu, H. Liu, Y. Wang, W. Yang, Z. Xie, W. Hua, Z.

© 2023 The Authors. ChemCatChem published by Wiley-VCH GmbH

Gao, *J. Catal.* **2008**, *258*, 243–249; i) F. L. Bleken, K. Barbera, F. Bonino, U. Olsbye, K. P. Lillerud, S. Bordiga, P. Beato, T. V. W. Janssens, S. Svelle, *J. Catal.* **2013**, *307*, 62–73.
[13] a) W. Schwieger, A. G. Machoke, T. Weissenberger, A. Inayat, T. Selvam, M. Klumpp, A. Inayat, *Chem. Soc. Rev.* **2016**, *45*, 3353–3376; b) M. Hartmann, A. G. Machoke, W. Schwieger, *Chem. Soc. Rev.* **2016**, *45*, 3313–3330; c) D. Verboekend, J. Pérez-Ramírez, *Catalysis Science, Technology* **2011**, *1*, 879–890.
[14] D. Freude, T. Fröhlich, M. Hunger, H. Pfeifer, G. Scheler, *Chem. Phys. Lett.* **1983**, *98*, 263–266.
[15] R. Caicedo-Realpe, J. Pérez-Ramírez, *Microporous Mesoporous Mater.* **2010**, *128*, 91–100.
[16] a) M. Dyballa, U. Obenaus, M. Blum, W. Dai, *Catalysis Science, Technology* **2018**, *8*, 4440–4449; b) M. Dyballa, U. Obenaus, S. Lang, B. Gehring, Y. Traa, H. Koller, M. Hunger, *Microporous Mesoporous Mater.* **2015**, *212*, 110–116.
[17] M. S. Holm, S. Svelle, F. Joensen, P. Beato, C. H. Christensen, S. Bordiga, M. Bjørgen, *Appl. Catal. A* **2009**, *356*, 23–30.
[18] a) K. Barbera, F. Bonino, S. Bordiga, T. V. W. Janssens, P. Beato, *J. Catal.* **2011**, *280*, 196–205; b) P. Sazama, B. Wichterlova, J. Dedecek, Z. Tvaruzkova, Z. Musilova, L. Palumbo, S. Sklenak, O. Gonsiorova, *Microporous Mesoporous Mater.* **2011**, *143*, 87–96.
[19] L. Lakiss, F. Ngoye, C. Canaff, S. Laforge, Y. Pouilloux, Z. Qin, M. Tarighi, K. Thomas, V. Valtchev, A. Vicente, L. Pinard, J.-P. Gilson, C. Fernandez, *J. Catal.* **2015**, *328*, 165–172.
[20] X. Zhou, C. Wang, Y. Chu, J. Xu, Q. Wang, G. Qi, X. Zhao, N. Feng, F. Deng, *Nat. Commun.* **2019**, *10*, 1961.
[21] a) Ł. Kuterasiński, U. Filek, M. Gackowski, M. Zimowska, M. Ruggiero-Mikołajczyk, P. J. Jodłowski, *Ultrason. Sonochem.* **2021**, *74*, 105581; b) A. Święs, A. Kowalczyk, B. Gil, L. Chmielarz, *RSC Adv.* **2022**, *12*, 9395–9403; c) H. Xin, X. Li, Y. Fang, X. Yi, W. Hu, Y. Chu, F. Zhang, A. Zheng, H. Zhang, X. Li, *J. Catal.* **2014**, *312*, 204–215; d) A. M. Varvarin, K. N. Khomenko, V. V. Brei, *Theor. Exp. Chem.* **2011**, *47*, 36–40.
[22] J. F. Souza de Carvalho Filho, M. Maciel Pereira, D. A. Gomes Aranda, J. Monnerat Araujo Ribeiro de Almeida, E. Falabella Sousa-Aguiar, P. Nothaft Romano, *Catalysts* **2019**, *9*, 617.
[23] J. W. Jun, Z. Hasan, C.-U. Kim, S.-Y. Jeong, S. H. Jhung, *J. Nanosci. Nanotechnol.* **2016**, *16*, 4377–4385.
[24] M. Dyballa, P. Becker, D. Trefz, E. Klemm, A. Fischer, H. Jakob, M. Hunger, *Appl. Catal. A* **2016**, *510*, 233–243.
[25] D. Müller, W. Gessner, H. J. Behrens, G. Scheler, *Chem. Phys. Lett.* **1981**, *79*, 59–62.
[26] a) A. J. J. Koekkoek, J. A. R. van Veen, P. B. Gerrtisen, P. Giltay, P. C. M. M. Magusin, E. J. M. Hensen, *Microporous Mesoporous Mater.* **2012**, *151*, 34–43; b) A. Omegna, J. A. van Bokhoven, R. Prins, *J. Phys. Chem. B* **2003**, *107*, 8854–8860; c) Z. Li, M. Benz, C. Rieg, D. Dittmann, A.-K. Beurer, D. Häussermann, B. Arstad, M. Dyballa, *Mater. Chem. Front.* **2021**, *5*, 4254–4271.
[27] a) Z. Li, D. Dittmann, C. Rieg, M. Benz, M. Dyballa, *Catalysis Science, Technology* **2022**, *12*, 2265–2277; b) Z. Li, D. Dittmann, C. Rieg, M. Benz, M. Dyballa, *Catalysis Science, Technology* **2022**, *12*, 5189–5202.
[28] a) D. Freude, M. Hunger, H. Pfeifer, W. Schwieger, *Chem. Phys. Lett.* **1986**, *128*, 62–66; b) H. Pfeifer, D. Freude, M. Hunger, *Zeolites* **1985**, *5*, 274–286; c) M. Hunger, *Solid State Nucl. Magn. Reson.* **1996**, *6*, 1–29.
[29] M. Dyballa, D. K. Pappas, K. Kvande, E. Borfecchia, B. Arstad, P. Beato, U. Olsbye, S. Svelle, *ACS Catal.* **2018**, *9*, 365–375.
[30] U. Olsbye, S. Svelle, M. Bjørgen, P. Beato, T. V. W. Janssens, F. Joensen, S. Bordiga, K. P. Lillerud, *Angew. Chem. Int. Ed.* **2012**, *51*, 5810–5831.
[31] C. Rieg, Z. Li, A. Kurtz, M. Schmidt, D. Dittmann, M. Benz, M. Dyballa, *J. Phys. Chem. C* **2020**, *125*, 515–525.
[32] C. Rieg, D. Dittmann, Z. Li, R. Lawitzki, K. Gugeler, S. Maier, G. Schmitz, J. Kastner, D. P. Estes, M. Dyballa, *Chem. Eur. J.* **2021**, *27*, 17012–17023.
[33] J. F. Haw, M. B. Hall, A. E. Alvarado-Swaisgood, E. J. Munson, Z. Lin, L. W. Beck, T. Howard, *J. Am. Chem. Soc.* **1994**, *116*, 7308–7318.
[34] Y. Jiang, J. Huang, W. Dai, M. Hunger, *Solid State Nucl. Magn. Reson.* **2011**, *39*, 116–141.
[35] J. Huang, N. van Vegten, Y. Jiang, M. Hunger, A. Baiker, *Angew. Chem. Int. Ed.* **2010**, *49*, 7776–7781.
[36] J. Huang, Y. Jiang, V. R. Reddy Marthala, W. Wang, B. Sulikowski, M. Hunger, *Microporous Mesoporous Mater.* **2007**, *99*, 86–90.
[37] C. Lieder, S. Opelt, M. Dyballa, H. Henning, E. Klemm, M. Hunger, *J. Phys. Chem. C* **2010**, *114*, 16596–16602.
[38] J. F. Haw, D. M. Marcus, *Top. Catal.* **2005**, *34*, 41–48.
[39] M. Rostamizadeh, F. Yaripour, *Journal of the Taiwan Institute of Chemical Engineers* **2017**, *71*, 454–463.
[40] T. V. W. Janssens, *J. Catal.* **2009**, *264*, 130–137.
[41] J. Schulz, F. Bandermann, *Chem. Eng. Technol.* **1994**, *17*, 179–186.
[42] D. Massiot, F. Fayon, M. Capron, I. King, S. Le Calvé, B. Alonso, J.-O. Durand, B. Bujoli, Z. Gan, G. Hoatson, *Magn. Reson. Chem.* **2002**, *40*, 70–76.

Manuscript received: June 2, 2023
Revised manuscript received: July 25, 2023
Accepted manuscript online: July 28, 2023
Version of record online: September 8, 2023

© 2023 The Authors. ChemCatChem published by Wiley-VCH GmbH